AIP | Review of Scientific Instruments

Electron current extraction from a permanent magnet waveguide plasma cathode

B. R. Weatherford, J. E. Foster, and H. Kamhawi

Citation: Rev. Sci. Instrum. **82**, 093507 (2011); doi: 10.1063/1.3642662
View online: http://dx.doi.org/10.1063/1.3642662
View Table of Contents: http://rsi.aip.org/resource/1/RSINAK/v82/i9
Published by the AIP Publishing LLC.

Electron current extraction from a permanent magnet waveguide plasma cathode

B. R. Weatherford,[1,a)] J. E. Foster,[1] and H. Kamhawi[2]
[1]*University of Michigan, Ann Arbor, Michigan 48109, USA*
[2]*NASA Glenn Research Center, Cleveland, Ohio 44135, USA*

(Received 6 April 2011; accepted 2 September 2011; published online 30 September 2011)

An electron cyclotron resonance plasma produced in a cylindrical waveguide with external permanent magnets was investigated as a possible plasma cathode electron source. The configuration is desirable in that it eliminates the need for a physical antenna inserted into the plasma, the erosion of which limits operating lifetime. Plasma bulk density was found to be overdense in the source. Extraction currents over 4 A were achieved with the device. Measurements of extracted electron currents were similar to calculated currents, which were estimated using Langmuir probe measurements at the plasma cathode orifice and along the length of the external plume. The influence of facility effects and trace ionization in the anode-cathode gap are also discussed. © *2011 American Institute of Physics*. [doi:10.1063/1.3642662]

INTRODUCTION

Plasma cathodes represent a class of electron sources that provide electrons via extraction through a sheath from a dense plasma source.[1] Electrodeless plasma discharge variants of this class of electron sources offer potential advantages relative to conventional hot electron sources. Unlike filaments or hollow cathodes, the emission surface is not a physical electrode. Rather, it is virtual in the form of an electrostatic sheath. This limits the wear on bounding surfaces, which extends useful operating lifetime and also avoids the contamination of thermionic emitters that can arise from electrode erosion. Such sources can operate on a variety of gases ranging from inert to highly oxidizing gases, making them applicable to a broad range of applications ranging from plasma processing to space propulsion. Indeed, the space propulsion application is the chief motivation for this work. Some missions that are envisioned, ion thrusters for example, will require operating times in excess of 5 years, making the issue of cathode lifetime critical.

Plasma cathodes may be a viable solution, but there are technical challenges, such as maximizing the extracted current-to-power ratio such that it is competitive with conventional hollow cathodes. The key to provide high extraction currents is the production of a dense plasma within the device. Helicon sources are capable of producing very high plasma densities and have been demonstrated in plasma cathode embodiments supplying tens of Amperes of electron current at high power.[2] Resonant microwave cavity discharge plasmas have also been investigated for cathode applications.[3] The work presented herein focuses on a microwave electron cyclotron resonance (ECR) plasma cathode approach.

ECR discharges have been studied as sources of single and multiply charged ions,[4–8] with more specific applications in plasma etching[8] and thin film deposition.[9,10] Over the years, ECR sources have matured into a reliable technology for a diverse set of materials processing applications.[11] One common attribute of ECR plasma sources is the ability to generate high density plasmas at pressures down to the submillitorr range. The efficient operation of ECR sources at low pressures makes them attractive for electric propulsion applications. The study of ECR-based ion thrusters dates back to the mid-1960s,[12] and has continued as an active area of research ever since.[13–15]

Some microwave ECR plasma cathodes have been investigated in the recent past,[16,17] and one design has actually been successfully demonstrated in space as an ion thruster neutralizer source on the Hayabusa asteroid-sample return mission.[15,18] The Hayabusa plasma cathode featured an antenna immersed in the ECR plasma. Such antennas are subject to erosion via ion bombardment and thus have a limited operational lifetime.[19]

The plasma cathode investigated in the work obviates the need for an internal excitation antenna. Instead, the plasma source in this work is essentially a microwave waveguide in which an external permanent magnetic circuit establishes the interior conditions for ECR heating to occur. Launched microwaves are absorbed at the established heating zones, breaking down the feed gas. Presented herein are operating characteristics of this source as well as plasma measurements used to understand how source plasma conditions change with operating parameters such as gas flow, extraction voltage, and input microwave power.

EXPERIMENTAL SETUP

A cross-sectional schematic of the plasma cathode is shown in Figure 1. The device mainly consists of a copper tube, 7.6 cm in diameter and 10.0 cm long, with two end flanges. The upstream end of the source is sealed with a 12.7 cm diameter, 0.6 cm thick quartz window, and an O-ring groove. Microwaves are launched through the window and into the source by a waveguide, mounted on the upstream end of the window. The use of traveling microwaves, as opposed

a)Author to whom correspondence should be addressed. Electronic mail: brweathe@umich.edu.

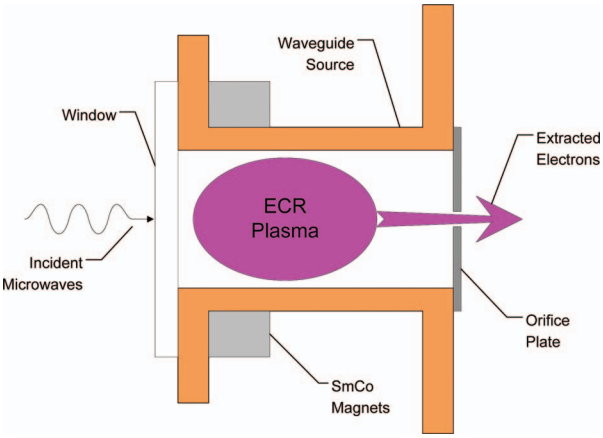

FIG. 1. (Color online) Schematic depiction of ECR plasma cathode.

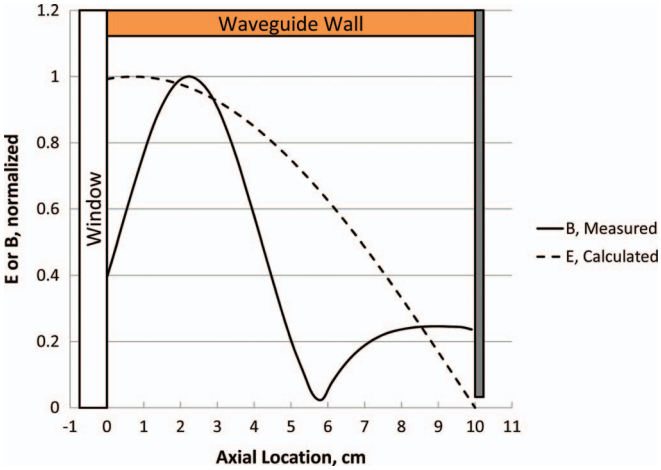

FIG. 2. (Color online) Microwave electric field and static magnetic field distributions within the waveguide plasma source.

to a driven microwave-frequency electric field near a launching antenna, places inherent size constraints on the waveguide. The TE mode is desired for ECR coupling to the on-axis axial magnetic field. The cutoff radius for a given mode TE_{nm} is given by

$$a_{c,nm} = \frac{p'_{nm}}{2\pi f\sqrt{\mu\varepsilon}}, \tag{1}$$

where $a_{c,nm}$ is the cutoff radius, f is the microwave frequency, μ and ε are the permeability and permittivity, respectively, of the material within the waveguide, p'_{nm} is the mth root of J'_n, and J'_n is the derivative of the nth Bessel function of the first kind.

The circular waveguide mode with the smallest cutoff radius at a given frequency is the TE_{11} mode. This mode contains an electric field pattern that is peaked on axis, oriented perpendicular to the axis, with one complete variation in the azimuthal electric field over π radians.[20] The source is designed to operate in the circular TE_{11} mode, as it allows for a waveguide radius greater than the cutoff radius for the TE_{11} mode but smaller than those for higher order modes. By choosing a radius that satisfies these constraints, mode competition from higher order modes is prevented. The geometry accommodates right hand circularly polarized (RHCP) wave heating, where the microwave electric field is perpendicular to the static magnetic field, and the wave propagation vector is parallel to the static magnetic field.

The magnetic circuit was designed in such a way to ensure that the region of strong applied microwave electric field coincides with the location of the 875 Gauss heating zone for 2.45 GHz microwaves. Since the electric field in the circular TE_{11} mode is strongest on the centerline of the waveguide, this magnetic field strength should ideally be located near the centerline as well. The orientation of the magnet rings is parallel to the waveguide axis, which sets up a predominantly axial magnetic field within the resonant heating zone, as required for RHCP wave propagation. An axial field profile of the microwave electric field and the measured magnetic field is shown is shown in Figure 2.

The magnets are held in place with aluminum clamps. The downstream end of the source allows for the mounting of interchangeable endplates with different extraction aperture diameters. The plasma cathode could be isolated from the vacuum facility using a teflon spacer and nylon fasteners, or grounded with the use of an aluminum spacer. Gas was injected into the source using an 8-aperture gas plenum ring located near the waveguide window, which also served as a vacuum seal. For the work presented herein, argon was the feed gas.

A magnetron was used as the microwave power source, and the output of the magnetron was connected directly to a power circulator. Incident and reflected microwave power levels were monitored by a 60 dB, two-way directional coupler and power meters. A three-stub tuner was used for load matching. A cylindrical to rectangular waveguide adapter was used to couple power from the three stub tuner to the cylindrical plasma cathode. The microwave input power setup is shown schematically in Figure 3. The plasma source was mounted on axis atop a cylindrical vacuum chamber, 62 cm in length and with an inner diameter of 42 cm, which served effectively as an exhaust vacuum dump. Gas flowing out of the plasma cathode enters the downstream chamber, which is evacuated by turbopump.

Diagnostics

Electron current was extracted from the source using a 12 cm-diameter molybdenum extraction electrode, located 14 cm downstream from the source. Extractable current acquired as a function of operating condition was monitored by biasing the plate and recording current as illustrated in Figure 4.

A cylindrical Langmuir probe was used to assess plasma properties both inside the source and at downstream locations.

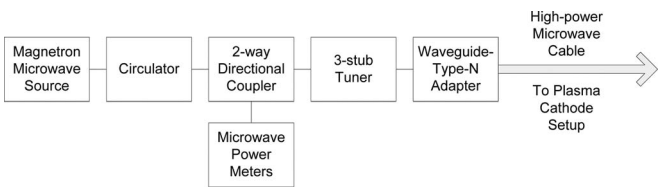

FIG. 3. Block diagram of the microwave power circuit.

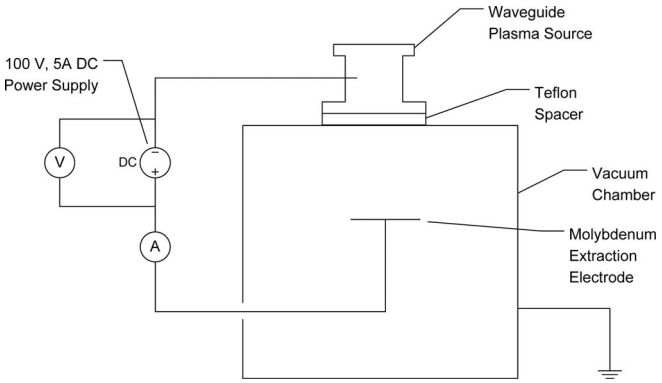

FIG. 4. Schematic of electron current extraction circuit.

To study the region between the plasma cathode aperture and extraction anode in more detail, a planar Langmuir probe was mounted on a translation stage and moved along the centerline of the chamber, within the anode-cathode gap. During the probe measurements and the teflon spacer was replaced with a metal spacer, grounding the plasma cathode to the vacuum facility. This had no significant effect on the performance of the device. Langmuir probe I-V characteristics were recorded using an automated data acquisition system.

EXPERIMENTAL OBSERVATIONS AND ANALYSIS

Initial current extraction—Open source

Baseline current extraction measurements, shown in Figure 5, were initially carried out without an extraction aperture; that is the end plate was absent. For this data set, argon gas flow into the source was varied from 3 sccm to 8 sccm. The bias voltage on the extraction plate was set at +100 V. Absorbed (forward minus reflected) microwave power was varied between 40 and 100 W. Reflected power always remained below 20 W and often was below 10 W. As expected, extracted current increased monotonically with increasing absorbed microwave power. The maximum extracted current was 0.52 A, at a flow rate of 8 sccm and 120 W of absorbed microwave power. As can be seen in Figure 5, extracted current is a monotonic function of flow rate. At a fixed flow, extracted current tends to increase and saturates at the higher powers. The observed dependence of current on gas flow is expected, as neutral density and thus total ionization rate should increase with flow rate. The relationship between extracted current and power at fixed flow may be related to plasma production in the ECR zone.

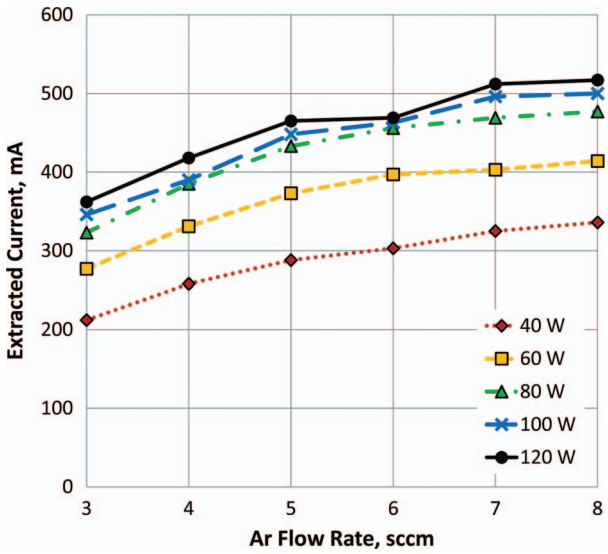

FIG. 5. (Color online) Extracted current vs. absorbed power and flow rate at 100 V, with open-ended source.

Because there is very little neutral containment in the open source, the majority of the extracted current is likely due to plasma produced at the ECR heating zone. At low pressure, that is without an extraction orifice, plasma production is localized at the heating zone. Once the neutrals in this region are depleted, the electron current cannot increase. This is consistent with neutral depletion studies as well as studies investigating the ionization efficiency of ECR discharges at low pressure. At low pressure, in particular, much of the energy goes into heating electrons. This raises the plasma potential in the heating zone, and energy is lost by ions falling through the sheath at the walls of the source. Ionization efficiency is, therefore, poor at such conditions. The key point is that ionization efficiency goes down at fixed flow once the input power exceeds that required to produce appreciable ionization in the heating zone, apparently 80 W in this case.[21,22]

Sensitivity to orifice size

One key consideration for plasma cathodes, particularly, those desired for space applications, is the minimization of the required flow rate to produce a desired emission current at minimal discharge power. In this regard, neutral containment is important. In the ideal case, neutral particles are recycled many times before ultimately escaping the source. By recycling, we refer to cyclic neutral particle ionization and subsequent neutralization at wall surfaces. A high recycling rate means that each neutral particle can supply many electrons before being ultimately lost from the device through the orifice. The problem of neutral containment can be looked at from a gas dynamic standpoint. Here, the total pressure within the plasma cathode is P_{source} and the exhaust chamber is at some pressure P_{exhaust}. Since the throughput and the pressure in the exhaust chamber are known, the pressure inside the source can be estimated, provided the conductance of the extraction aperture is known. The conductance, C, of a thin aperture assuming free molecular flow may be expressed as

$$C = \frac{v}{4}A, \tag{2}$$

where v is the mean thermal speed of the argon atom, and A is the area of the orifice. The relationship between the internal source pressure, exhaust chamber pressure, and the throughput, Q, may be expressed as,

$$Q = C\,(P_{\text{source}} - P_{\text{exhaust}})\,. \tag{3}$$

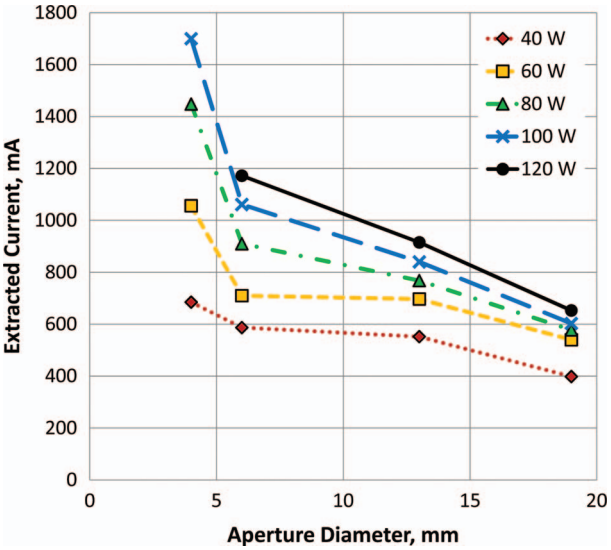

FIG. 6. (Color online) Extracted current vs. aperture size, at 80 V and 5 sccm.

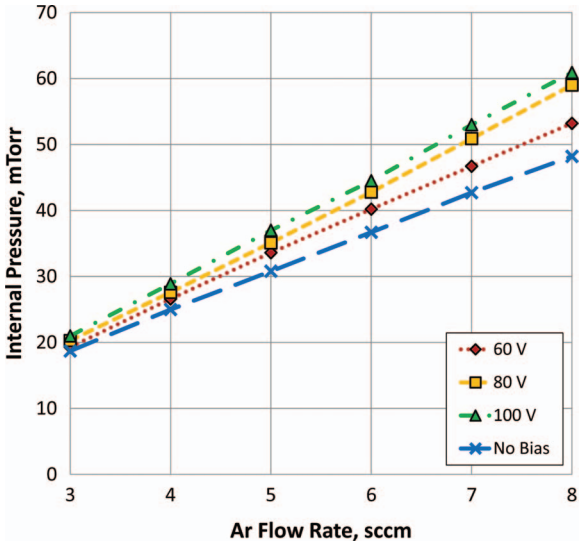

FIG. 7. (Color online) Measured internal pressure with 4 mm aperture, at 120 W of absorbed microwave power.

If there is no significant heating of the neutral gas and the average ionization fraction over the volume of the plasma cathode is sufficiently low, then the internal pressure should vary linearly with flow rate by Eq. (3).

Increasing the neutral density is one method of improving source ionization efficiency. Rather than simply increasing the gas flow, internal pressure within the source can be increased by terminating the exit plane with plate with an aperture. In this work, four different aperture sizes were studied. Each aperture plate was made from steel sheet metal with a thickness of 0.6 mm. The aperture sizes investigated were 19 mm, 13 mm, 6 mm, and 4 mm in diameter. The extractable current was measured using the downstream collector plate described previously at a bias of 80 V. As can be seen in Figure 6, there is an inverse relationship between orifice size and extracted current over the entire power range investigated. The effect is most dramatic at the higher power levels.

Figure 6 appears to indicate that ionization efficiency does indeed increase with reducing orifice size as discussed earlier. The slope in all cases increases when transitioning from the 6 mm to the 4 mm aperture, and the sensitivity with respect to microwave power increases.

This change with the small orifice most likely indicates increased ionization within the source. One possible source of the increased ionization is plasma production within the source, derived from ECR-produced electrons streaming under the influence of the applied electric field. Measurements of the internal pressure with the 4 mm aperture are shown in Figure 7, and as expected, the pressure varies linearly with respect to flow rate. At 80 V, the measured pressure was 36 mTorr with the 4 mm orifice, while the (calculated) pressure with the 19 mm orifice is roughly 2 mTorr. The ionization pathlength (assuming a cross-section of 4×10^{-16} cm^2) in the 19 mm case is then on the order of tens of centimeters, larger than the plasma cathode dimensions. With the 4 mm aperture, the ionization pathlength drops to roughly 2 cm. This is shorter than the source dimensions, so additional ionization within the plasma cathode is more likely, and the increased impact ionization within the source itself is likely the primary contributor to the change in slope.

Performance with 4 mm aperture

The 4 mm orifice was further studied to investigate the sensitivity of extractable current to extraction voltage. A photograph of the plume produced between the extraction aperture and the collector plate at an extraction voltage of 80 V is shown in Figure 8. The collimated beam is readily observable suggesting collisional excitation of the background gas by the electron beam. It should be pointed out that the relaxation of exited ions and neutrals exiting the source is not a plausible explanation for the plume. Neutral velocities are ~300 m/s and relaxation times are of order 10^{-8} s, so that distance traveled before the emission of a photon is of order very small fractions of a millimeter.

The collimating effect of the exit orifice assures that the neutral density on axis, in the exhaust chamber, will be higher than far removed off-axis points. Following this reasoning,

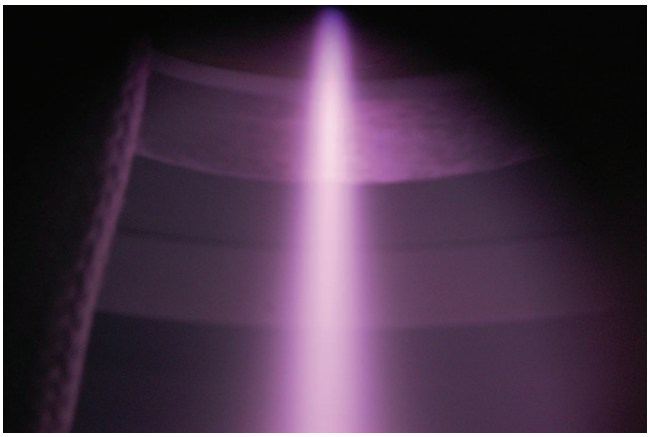

FIG. 8. (Color online) Photograph of plume from the plasma source, with 4 mm aperture.

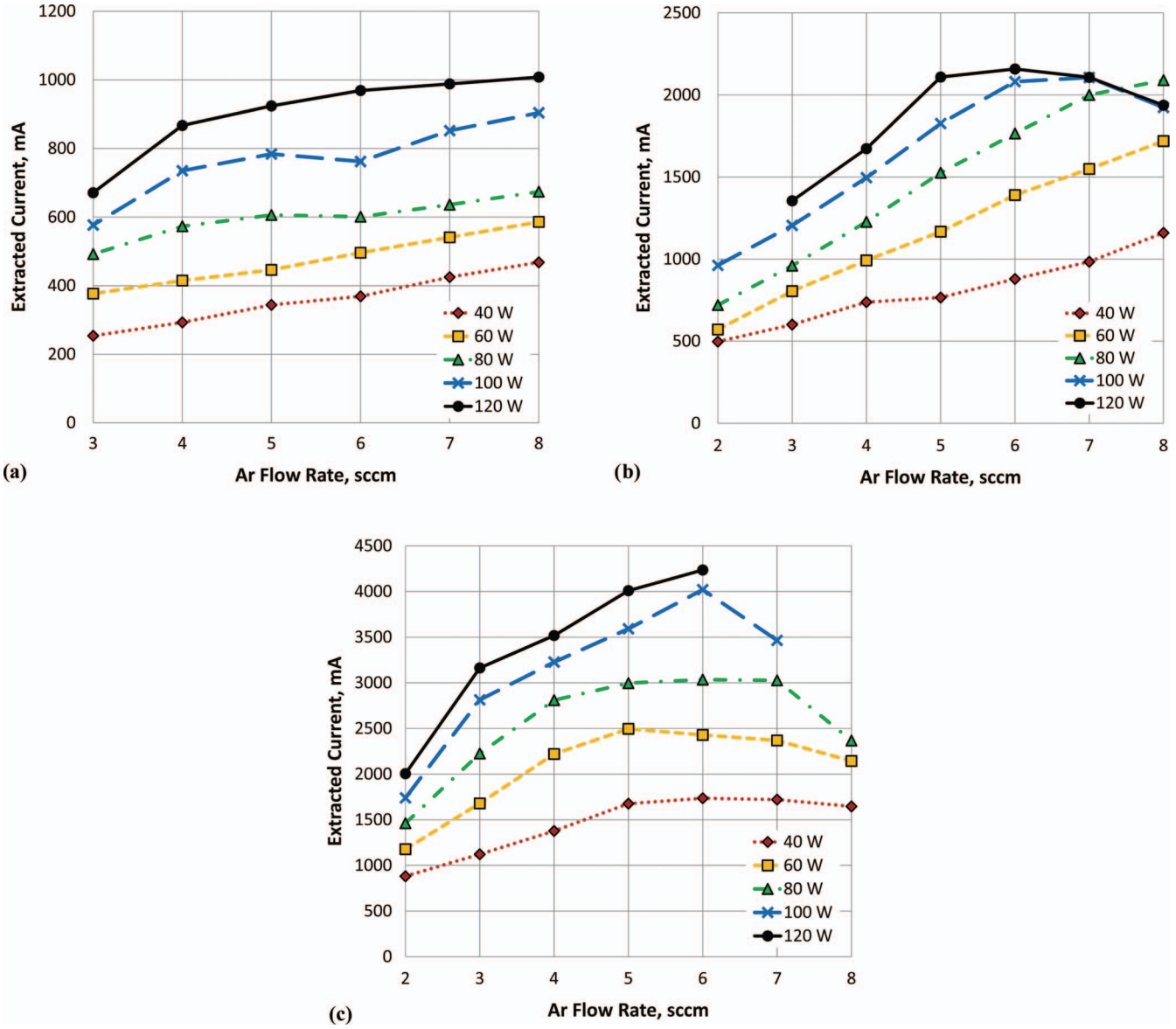

FIG. 9. (Color online) Extracted electron current, with 4 mm aperture. Extraction bias of (a) 60 V, (b) 80 V, and (c) 100 V.

then in order for electrons to produce the observed excitation, they must exit the plasma cathode with appreciable energies.

The extracted current with the 4 mm aperture was measured as a function of argon flow rate and absorbed microwave power, with extraction electrode biases of 60 V, 80 V, and 100 V. The results are plotted in Figure 9. The maximum amount of extractable current attained over the limited power range investigated was 4.24 A, which was achieved at 6 sccm, 120 W of microwave power, and an extraction bias of 100 V. The plots shown in Figure 9 yield a great deal of insight into plasma production and electron extraction in the source. At a fixed extraction voltage, it can be seen that at fixed flow rate, the extractable current increases with increasing microwave power. This is consistent with the electropositive model for plasma discharges where the plasma density is a linear function of input power. Additionally, as expected in low pressure discharges, the current also tends to increase with flow rate. The character of this behavior changes with increasing bias voltage. At the higher voltages, at a given flow rate, the current actually saturates at high microwave power. For example, at 80 V dc extraction voltage, the current saturates at around 2000 mA at flow rates greater than 5 sccm. But a mere increase in extraction voltage of 20 V to a total of 100 V extends the current range from a maximum around 2000 mA at 80 V to over 4000 mA at 100 V. Indeed, for a given microwave power, higher currents are seen as the voltage increases, regardless of the flow rate. This point supports that the dc field may act as an important current "amplifier" of electron flux extracted from the ECR region.

An interesting observation can be made regarding the variation in current with flow at extracted currents above 2000 mA. For those cases where the current has reached 2000 mA, the current tends to level off with increasing flow, essentially saturating and in some cases actually decreasing with flow rate. This can be observed in both the 80 V and 100 V case. This behavior is likely due to space charge limitations. As will be discussed later, at lower extraction voltages, the extracted current is smaller and tends to increase

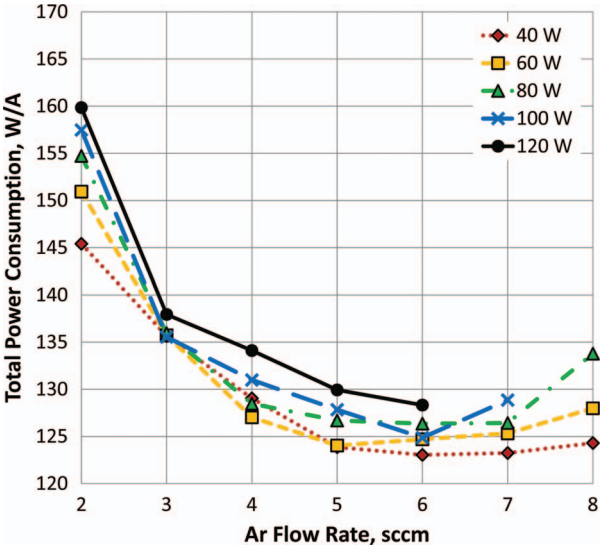

FIG. 10. (Color online) Total (microwave + beam) power consumption, 100 V bias.

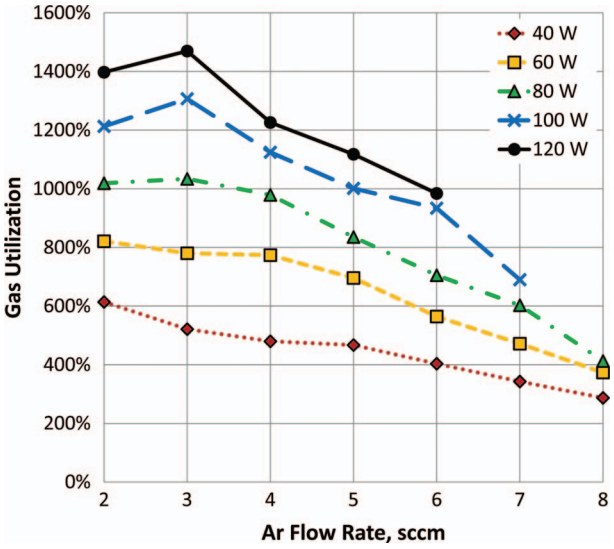

FIG. 11. (Color online) Gas utilization factor, at 100 V bias.

monotonically with flow. The current increase is due to variation of the impact ionization rate inside the source, which increases as neutral gas density (via pressure) is increased. As input microwave power is increased at a fixed bias, the internal ionization rate from ECR heating increases, leading to higher current.

However, once the extracted current approaches the space charge limit, the extracted current is reaches its maximum. The extracted current must be transported over a large gap and is thus inherently space charge limited. In addition to determining the space charge limit, a high bias increases the likelihood of ionization external to the source. This ionization reduces space charge effects allowing for more current to be transported. This latter effect would tend to be more effective at the higher currents, as is illustrated by Figure 9(c).

Figure 10 shows the ratio of total input power to extracted current, known as the electron production cost, plotted as a function of flow rate. As can be seen here, the electron production cost decreases with flow up to 6 sccm. This is reasonable, as ionization rate is proportional to neutral density, and the extracted current at these flow rates is not at the space charge limit. Beyond 6 sccm, the extracted current is presumably space charge limited. The extracted current in this range is decreasing with gas flow, due to a combination of electron cooling via electron-neutral collisions and space charge limited operation.

Another parameter that yields insight on the discharge efficiency is the ratio of the emission current to the gas flow rate measured in equivalent Amperes. This parameter, known as the gas utilization, is a measure of how many electrons are produced per injected neutral particle and roughly indicates the number of times a neutral particle is recycled before ultimately being lost from the plasma cathode. Figure 11 illustrates the dependence of utilization on flow rate. The gas utilization decreases precipitously with increasing gas flow and appears to converge toward a utilization of 300% at high flow rates, independent of microwave power level. This behavior is again suggestive of space charge limitations. When the bias is fixed and flow is varied, as in Figure 9, the current cannot increase monotonically with increasing flow rate. So at higher flow rates, Figure 10 suggests that the discharge efficiency is limited.

Internal plasma measurements

Langmuir probe measurements were also acquired in this work. The measurement locations included the region inside the source but downstream of the ECR zone, measurements within the aperture region, and measurements within the plume. The internal probe was located at the downstream end of the plasma cathode, ~1.1 cm off-axis. This probe was used to measure the internal plasma density produced by the ECR source discharge via the ion saturation current. Plasma measurements gave densities from 9×10^{10} cm^{-3} at 3 sccm to 3.4×10^{11} cm^{-3} at 8 sccm, with an applied bias of 80 V. These densities are well in excess of that which would be expected based on cutoff considerations at 2.45 GHz (7×10^{10} cm^{-3}), suggesting that at least in the ECR zone, overdense plasma may have been produced.

Probe data—Plasma properties in plume

Langmuir probe measurements provide some insight on electron multiplication in the plume. A cylindrical probe used to study the dependence of external plasma density on applied bias. The cylindrical probe was .51 mm in diameter, and 3.0 mm long, and was oriented perpendicular to the waveguide axis, 43 mm downstream from the extraction aperture. The exposed probe tip was placed so that it was centered within the visible plume, and probe traces were taken as the anode bias was varied.

Impact ionization by electrons in the plume would increase the electron density above the expected value, calculated from conservation of flux, as electrons are accelerated across the gap. The electron flux leaving the orifice may be expressed as: $\Gamma_0 = n_0 v_0$. Here, Γ_0, n_0, and v_0 are the electron flux, density, and velocity in the orifice, respectively. If

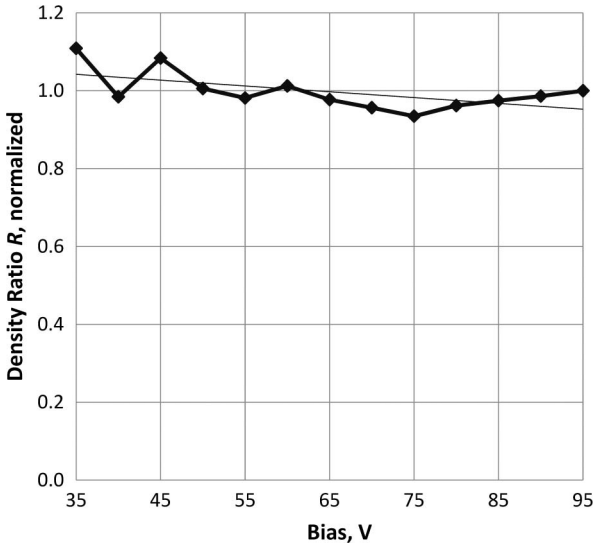

FIG. 12. Normalized ratio, R, of measured density to density calculated from current and accelerating voltage, at 6 sccm and 60 W.

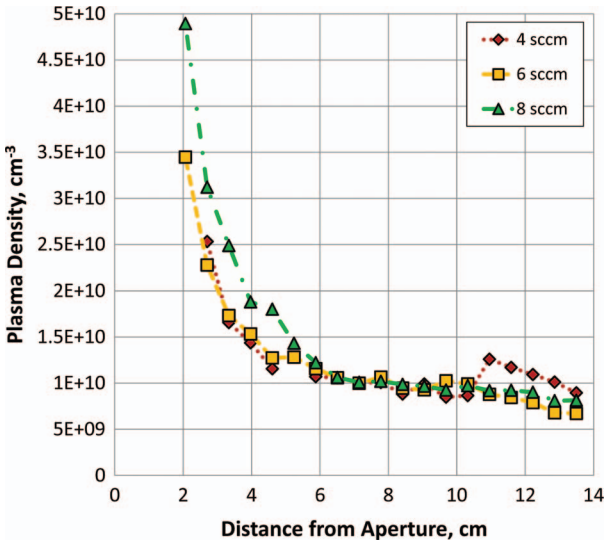

FIG. 13. (Color online) Plasma density along length of the plume, at 60 V and 60 W.

there is no appreciable multiplication in the plume, then the flux is proportional to the current, I. Then, the density measured by the probe just downstream of the source should scale as $I/\sqrt{V}$, where V is the bias voltage. It is assumed that the accelerating voltage is proportional to the actual applied voltage. For relatively unimpeded electron transport to the biased plate, the density ratio R

$$R = n_e \frac{\sqrt{V}}{I}, \tag{4}$$

should, therefore, be a constant. Variation in this ratio with respect to voltage suggests that the occurrence of either plume ionization or depletion is a significant source or sink of the electrons that are collected by the anode.

Figure 12 shows the normalized density ratio, R, at 60 W and 6 sccm. As seen in the figure, there is little variation in this parameter, particularly, at voltages beyond 60 V. This suggests that the downstream density is well described by simple plume expansion due to acceleration and conservation of flux. Therefore, it is unlikely that electron multiplication through impact ionization in the plume is a significant source of collected electrons.

A planar probe, 3.2 mm in diameter, was used to map out a series of probe traces on centerline between the orifice and external anode. During these measurements, the pressure in the exhaust chamber was 0.25 mTorr, the microwave power was 60 W, and the anode bias was 60 V.

The resulting plasma density from ion saturation current is shown in Figure 13, while the plasma potential is in Figure 14. The plasma density drops off rapidly within the first few centimeters from the orifice, and at all flow rates, reaches a value of roughly 10^{10} cm^{-3} near the anode surface ($z = 14$ cm). Traces were not recorded any closer than 2 cm from the aperture, where the probe body blocked the aperture and the plume was extinguished, but it is reasonable to expect even higher plasma densities in the aperture.

The plasma potential profiles suggest that the plasma plume is nearly quasineutral, with a plasma potential within 15–20 V below the anode bias. There is a small electric field (0.4 V/cm) over the length of the plume, ascertained by fitting a line to the plasma potential profile. In this sense, the plume resembles the positive column of a glow discharge. Assuming an electron-neutral elastic scattering rate constant of 10^{-7} cm^3/s, [23] the corresponding electron mobility is 2.17×10^5 m^2/V-s. If the 10^{10} cm^{-3} electron density is taken at the anode surface, the electric field in the plume drives a current density of $\sim$1.3 A/cm^2 at the anode. Given a factor of two uncertainty in the density measurement, this result corresponds well with the observed currents and beam sizes on the order of 0.5–3 cm in diameter.

While ionization outside the source may be essential for establishing the plume plasma and avoiding space charge limitations, this trace ionization does not directly supply electrons to the anode. The ionization pathlength at the typical background pressure of 0.5 mTorr is roughly 1.5 m (assuming

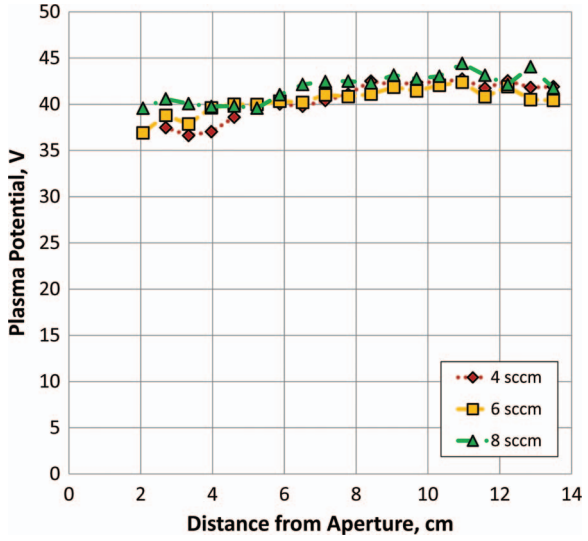

FIG. 14. (Color online) Plasma potential along length of the plume, at 60 V and 60 W.

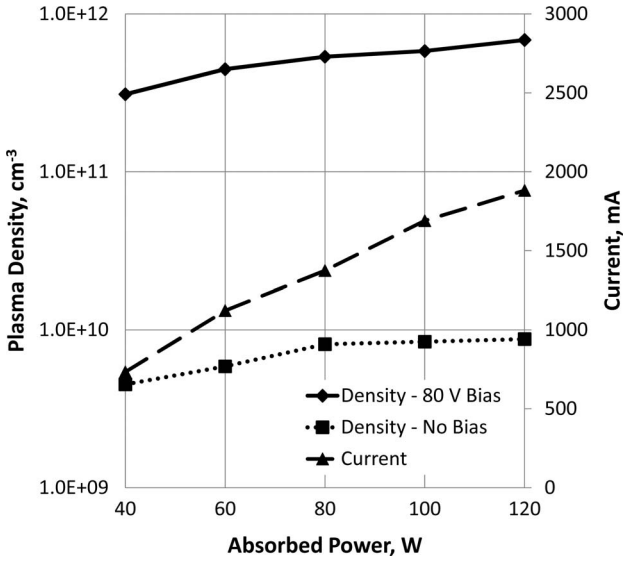

FIG. 15. Plasma density in orifice, at 6 sccm, with and without 80 V bias.

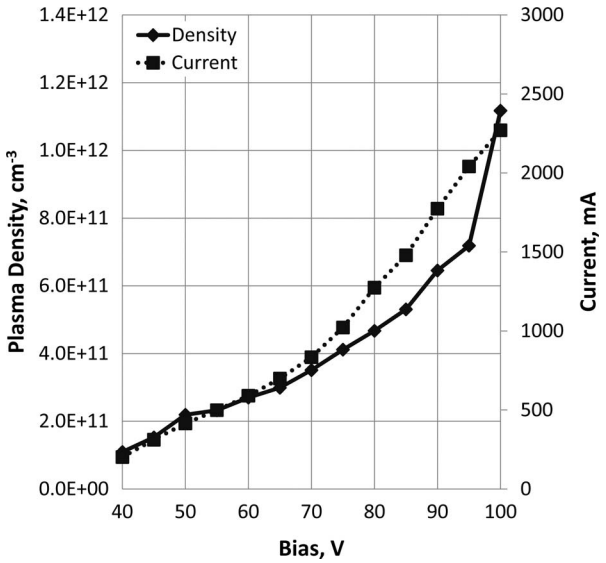

FIG. 16. Plasma density within orifice and extracted current, at 6 sccm and 60 W.

the peak ionization cross-section), while the anode-cathode gap is 14 cm. To the first order, this implies that at most, 9% of the electrons leaving the aperture undergo ionization collisions.

Probe data—Orifice plasma density

Of particular interest is the effect of the applied bias on plasma production and electron extraction in the vicinity of the extraction orifice as this region defines the electron emission surface. Langmuir probe measurements were taken at a fixed position within the extraction aperture. The probe tip was aligned with the source axis and centered in the orifice. The probe tip had a length of 9.53 mm and a diameter of 0.28 mm. The probe body was situated so that 5 mm of the probe tip was located downstream from the aperture, with the remainder of the probe tip inside the aperture and the plasma source. In this regard, the probe measurement represents the average plasma properties in the orifice region. Probe data were acquired at variable microwave power levels and 80 V extraction bias. The plasma density measured within the orifice at 6 sccm is shown in Figure 15.

Without an applied bias, the orifice plasma density varies from 4.5×10^9 cm^{-3} to 8.8×10^9 cm^{-3}. When an 80 V bias is applied, at the same microwave power levels, the density varies from 3.1×10^{11} to 6.8×10^{11} cm^{-3}, a jump in plasma density of nearly a factor of 100. The data shown here indicate that bias voltage plays a significant role in plasma production and subsequent electron emission in the orifice region. Without the bias voltage, plasma density is low, presumably because electron flow is due to diffusion from the ECR heating zone to the extraction aperture. As suggested by the data, electric field-driven impact ionization inside the source may play a major role in attaining large extraction currents.

Figure 16 shows the plasma density in the orifice and extracted current as a function of bias, at 6 sccm and 60 W. The plasma current and density monotonically increase with increasing voltage. This trend is consistent with impact ionization under the influence of the applied electric field. The rate of increase is greater, however, between 65 V and 90 V. Interestingly, the behavior of the current with respect to voltage closely follows the Child-Langmuir scaling, as shown in Figure 17. As shown by the probe measurements in Figures 13 and 14, external plasma formation via trace ionization can mitigate space charge effects over the majority of the gap. However, the extraction sheath at the orifice may still impose the space charge limit over the sheath thickness. For a 4 A beam, for example, assuming an extraction sheath potential of 40 V at the 4 mm aperture, the Child-Langmuir sheath thickness would be .004 cm. This is entirely reasonable, as it corresponds to the Debye length of an orifice plasma at 10^{11} cm^{-3} and an assumed temperature of 4 eV. It appears

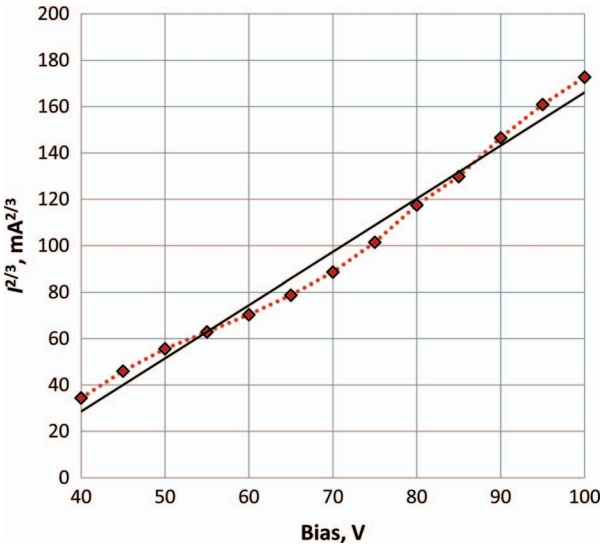

FIG. 17. (Color online) Measured current, with linear overlay, demonstrating space charge limited current behavior, at 6 sccm and 60 W.

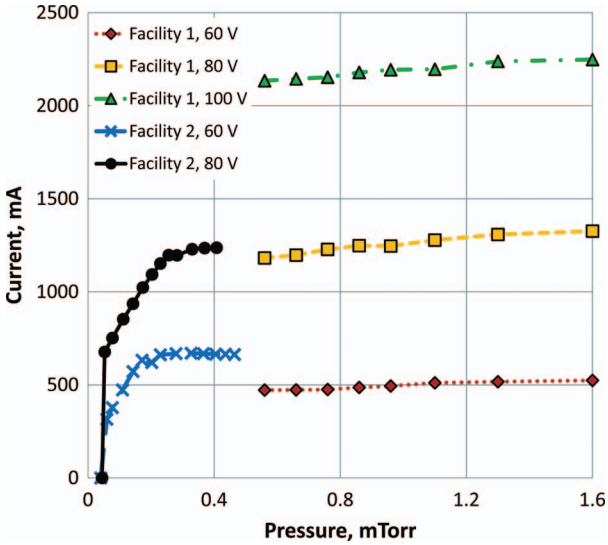

FIG. 18. (Color online) Effect of background argon pressure on extracted current, 6 sccm source flow, 60 W.

that in some cases, saturation effects at fixed voltage can be interpreted as simple space charge limited flow.

Investigation of facility effects

Extracted electron current is collected by the downstream electrode. Accompanying the current flow is a luminous plume visible between the plasma cathode and the collector plate as shown in Figure 8. Presumably, the luminous plume is due to excitation of background gas in the gap between the plasma cathode and the collector plate. The amount of plasma production in the plume is a function of electron energy, which is directly tied to extraction voltage and background pressure. Previous discussion indicated that plume ionization is not a direct contributor to the extractable current. To assess the sensitivity of the magnitude of extracted current to plume ionization, the effect of chamber background pressure on collected current was investigated.

To carry out this sensitivity test, a second gas feed was connected directly to the vacuum chamber, and while keeping the flow rate through the plasma cathode constant; the flow rate of argon into the chamber was varied. This test was carried out in two facilities and results are shown in Figure 18. As can be seen in the figure, above 0.5 mTorr, the background pressure has little effect on extracted current. In this regard, it appears that any trace ionization produced with increasing voltage may just affect the space charge limit, rather than contributing significantly to the electron flux at the extraction anode. However, some minimal amount of external neutral gas may be required in order to form the bridge plume from the plasma cathode to the anode for this reason. The current extraction data presented in this work was acquired above this minimum, at pressures around 0.5 mTorr.

CONCLUDING REMARKS

The operation and plasma characteristics of the waveguide microwave ECR plasma cathode were investigated. Electron currents up to 4.2 A were extracted from the permanent magnet electron source with argon as the working fluid. This current level exceeds ion beam neutralization requirements for state of the art ion thrusters such as the NEXT engine. The data suggest that increased plasma density in the orifice accounts for the observed current increases with the anode bias voltage. During current extraction, high density plasma was observed within the source and at the extraction aperture. Langmuir probe traces in the plume suggest that electron flux is generally conserved in the plume, but a trace degree of ionization may be necessary to prevent space charge buildup in the anode-cathode gap. The plasma in the orifice region and at the anode was of sufficient density to account for the magnitude of collected electron current. The extracted electron flow was found to be space charge limited, which likely arises at the electron extraction sheath at the orifice.

[1]E. M. Oks, Plasma Sources Sci. Technol. **1**, 249 (1992).
[2]B. Longmier and N. Hershkowitz, Rev. Sci. Instrum. **79**, 093506 (2008).
[3]K. D. Diamant, IEEE Transactions on Plasma Science **37**(8), 1558 (2002).
[4]N. Saduko, K. Tokiguchi, H. Koike, and I. Kanomata, Rev. Sci. Instrum. **48**(7), 762 (1977).
[5]M. Dahimene and J. Asmussen, J. Vacuum Sci. Technol. B **4**(1), 126 (1986).
[6]L. Mahoney, M. Dahimene, and J. Asmussen, Rev. Sci. Instrum. **59**(3), 448 (1988).
[7]R. Geller, IEEE Transactions on Nuclear Science **23**(2), 904 (1976).
[8]J. Hopwood, M. Dahimene, D. K. Reinhard, and J. Asmussen, J. Vacuum Sci. Technol. B **6**(1), 268 (1988).
[9]G. Loncar, J. Musil, and L. Bardos, Czech. J. Phys. B **30**, 688 (1980).
[10]T. Roppel, D. K. Reinhard, and J. Asmussen, J. of Vacuum Sci. Technol. B **4**(1), 295 (1986).
[11]J. Asmussen, T. A. Grotjohn, P. Mak, and M. A. Perring, IEEE Transactions on Plasma Science **25**(6), 1196 (1997).
[12]D. B. Miller and E. F. Gibbons, AIAA J. **2**(1), 35 (1964).
[13]D. A. Kaufman, D. G. Goodwin, and J. C. Sercel, *Proceedings 29th AIAA/SAE/ASME/SAE Joint Propulsion Conference and Exhibit, Monterey, CA*, 28–30 June, 1993, AIAA Paper 1993–2108.
[14]J. E. Foster, T. Haag, H. Kamhawi, M. Patterson, S. Malone, F. Elliot, G. J. Williams, J. S. Sovey, and C. Carpenter, *Proceedings 40th AIAA/ASME/SAE/ASEE Joint Propulsion Conference and Exhibit, Ft. Lauderdale, FL*, 11–14 July, 2004, AIAA Paper 2004–3812.
[15]H. Kuninaka, K. Nishiyama, I. Funaki, T. Yamada, Y. Shimizu, and J. Kawaguchi, J. Propul. Power **23**(3), 544 (2007).
[16]H. Kamhawi, J. E. Foster, and M. J. Patterson, *Proceedings 40th AIAA/ASME/SAE/ASEE Joint Propulsion Conference and Exhibit, Ft. Lauderdale, FL*, 11–14 July, 2004, AIAA Paper 2004–3819.
[17]K. D. Diamant, *Proc. 31st International Electric Propulsion Conference, Ann Arbor, MI*, 20–24 September , 2009, Paper No. IEPC-2009–015.
[18]H. Kuninaka and S. Satori, J. Propul. Power **14**(6), 1022 (1998)
[19]S.-W. Kim, Y. Itoh, S. Satori, H. Okamoto, T. M. Sugiki, T. Kizaki, and M.-R. Nam, *Proceedings 40th AIAA/ASME/SAE/ASEE Joint Propulsion Conference and Exhibit, Fort Lauderdale, FL*, 11–14 July 2004, AIAA Paper 2004–4126.
[20]D. M. Pozar, *Microwave Engineering*, (Wiley, New York, 2005).
[21]A. Aanesland and A. Fredriksen, J Vac. Sci. Technol. A. **19**(5), 2446 (2001).
[22]M. Liu *et al.*, Plasma Sources Sci. Technol. **11**, 260 (2002).
[23]M. A. Lieberman, *Principles of Plasma Discharges and Materials Processing* (Wiley, New York, 2005).